

Refining the Model of Ionic Wind Propulsion

by Analyzing Thrust Dependence on

Electrode Geometry

Ryan Doel

A capstone report submitted to the faculty of
Brigham Young University
in partial fulfillment of the requirements for the degree of

Bachelor of Science

Bryan Peterson, Associate Research Professor

Department of Physics and Astronomy

Brigham Young University

Copyright © 2018 Ryan Doel

All Rights Reserved

ABSTRACT

Refining the Model of Ionic Wind Propulsion by Analyzing Thrust Dependence on Electrode Geometry

Ryan Doel

Department of Physics and Astronomy, BYU
Bachelor of Science

A single-stage parallel wire ionic wind device was investigated in an effort to further elucidate thrust dependencies. An attempt to measure the strength of the relationship between the geometrical constant C and the ratio of the emitter and collector diameters, $C \propto \frac{d_e}{d_c}$, was undergone. Consequently a 1m long assembly was created wherein electrode gap distance, applied voltage, and diameter of emitter and collector wire were varied. We found that the collector size has a larger impact on thrust than emitter diameter. It was observed that the lengthened device reduced end effects witnessed by other researchers. The relationship $C \propto \frac{d_e}{d_c}$ was never quantified due to the propagation of errors in our results. In an effort to reduce these errors, future research should acquire force measurements at 30+ different voltages for each configuration. Also, further studies should combine 4+ collector sizes and 4+ emitter sizes, in order to paint a broader picture of the force dependence on electrode size.

Keywords: [Electrohydrodynamics, Corona discharge, Ion wind, Single-stage, Ionic lifter]

ACKNOWLEDGMENTS

This research was supported by the Physics and Astronomy Department at Brigham Young University. I would like to thank Dr. Bryan Peterson for his unyielding encouragement and support, without which this project would have never gotten off the ground. I am also grateful for a patient and loving wife who encouraged my efforts throughout this project.

Contents

| | |
|----------------------------------|-----------|
| Table of Contents | iv |
| Introduction | 1 |
| Methods | 4 |
| Theoretical background | 4 |
| Experimental setup | 5 |
| Results and discussion | 8 |
| Conclusion | 12 |
| Bibliography | 14 |

Introduction

Ionic wind was originally discovered by Francis Hauksbee in 1709 AD who described the effect as a “weak blowing sensation” when an electrically charged tube was held close to him [1]. The phrase “ion wind” or “ionic wind” is the colloquial term used to describe the resulting flow of a medium—usually air—caused by a high potential difference between two conductors. This process is also known and studied as the Electrohydrodynamic effect (EHD). More specifically, the ion wind effect is caused by the onset of corona discharge. At the electrode distance I will be studying (primarily $d > 6$ cm), streamers created by the propagation of electron avalanches due to the ionization of the surrounding atmospheric air are initiated by the potential applied between the electrodes [2]. These ions then move along the electric field lines colliding with neutral molecules along their way. Each ion-neutral collision imparts momentum to the surrounding air, resulting in a wind-like flow of air which thrusts the EHD device in the opposing direction. This phenomenon has been applied to air purification, cooling of electronics [3], and optimistically theorized as the primary mode of propulsion for small aerial drones [4]. Previous work has elucidated a relationship between force and current, spacing of electrodes, and applied potential [4] [5]. Experiments have studied this effect with apparatuses submerged in nitrogen and argon gas at low and atmospheric pressure [6] [7].

Numerical simulations have tested the force dependence on changes in the collector¹ radius [8]. Various geometrical configurations have been studied: asymmetrical parallel wires [4] [9] [5] [10], cylinder-plate, wire-cylinder-plate [11], and pin-wire [12]. In addition to electrode geometry, effects of multiple staged devices have been studied [4] [13]. While the fundamental geometry we chose to study is not unfamiliar, single stage parallel wires, the three aims of our research are unique.

First, we experimentally prove parts of the theory presented. We make valuable commentary on how we sought to show how $C \propto \frac{d_e}{d_c}$ but failed to do so due to propagation of errors of successive fits to results.

Second, we verify the results produced by [4] as well as compare our results to [9], [10], and [5]. These four, single stage parallel wire, experiments used electrodes with respective lengths of 40 cm, 30 cm, 39 cm and 15 cm. Our setup allowed electrodes 1 m in length. [4] reported some results which defied theory and attributed the deviation to ‘end effects’. Within the theory we assume infinitely long electrodes, but at a sufficiently large electrode gap distance d , that assumption becomes invalid. Our experimental setup was designed to minimize these possible end effects, over the range of gap distances investigated by [4], and allow for more accurate results by using electrodes 1 m in length. Furthermore, we seek to make valuable comment on the comparison of results initiated by [9].

Third, we investigate how thrust varies upon the size of both the emitter and collector. While some extensive research in regards to electrode size [7] [8] [10] [9] has been conducted, few have varied both the emitter and collector size and elucidated their relationship with thrust. As will be shown in the theory section of this paper, the force produced is inversely proportional to the ion

¹While it is common to refer to parts of the electrodes as anode and cathode, the author abandons this terminology since it adds useless ambiguity. Typically the anode is associated with a positive voltage to which electrons flow and the cathode is associated with a negative voltage from whence electrons flow. The flow of ions in field case is not limited to the usual cathode to anode direction, thus we refer to the electrode at which the highest electric field density is found (the wire with the smallest diameter) as the emitter and the other (the wire with the larger diameter) as the collector.

mobility. Experimentally, we show how the ion mobility depends on the size of the emitter and collector.

Methods

Theoretical background

In this section we aim to produce the mathematical theory of ionic wind thrust production. Where ρ is the charge density of ions created by the corona discharge and v_d is the drift velocity of the ions. The current density is given by

$$j = \rho v_d = \rho \mu E \quad (1)$$

where μ is the ion mobility and E is the strength of the electric field. The current is consequently

$$I = \int j \cdot dA = \int \rho \mu E \cdot dA = \rho \mu EA \quad (2)$$

where A represents the cross sectional area of which the ions pass through toward the collecting region. The force these ions impart to the surrounding neutral air is equal to the force the electric field exerts on the ions which is given by

$$F = \int \rho E dV = \int_0^d \rho EA \cdot dx = \rho EAd = \frac{Id}{\mu} \quad (3)$$

where d is the distance between the emitter and collector: we refer to this often as the gap distance or electrode spacing. Now it is also known that the current dispensed from a corona discharge depends quadratically on the voltage applied between the electrodes [2].

$$I = CV(V - V_o) \quad (4)$$

where C is an empirical constant dependent upon device geometry and V_o is the corona inception voltage, the voltage required for corona discharge to begin. Upon combining the result of (3) and (4) and assuming that $C \propto \frac{\mu}{d^2}$ we find

$$F = \frac{CV(V - V_o)d}{\mu} = \frac{C_oV(V - V_o)}{d} \quad (5)$$

and once again C_o is a constant dependent upon the geometry of the lifting device.

Experimental setup

Our setup is an extension of that used by [4] and [5] and is shown in Fig. 1. A hanging assembly 1 m in length was suspended by nylon thread from a calibrated digital scale with 0.01g resolution and a max limit of 3 kg. The force measurement was obtained via a difference in weight of the hanging parallel wire assembly. The emitter voltage was applied from a 0 – (-80) kV RHR Spellman power supply with 1 mA current capability and the collector was physically grounded. While the method for breakdown and creation of ions varies upon polarity and distance between electrodes [2], it was reported by [5] that a negative applied voltage creates an effect indistinguishable from that caused by a positive voltage where $d \geq 3$ cm. Even so, when $d = 2$ cm the variation is minimal, thus the results presented generally hold for either polarity. Four different sized emitters ($d_e = 2.02$ mm, 1.02 mm, 0.65 mm, 0.2 mm) in combination with two different collectors ($d_c = 19$ mm, 6.4 mm) were used. Wire diameter measurements were made using a digital caliper with 0.01 mm resolution. The use of emitters and collectors more similar in diameter, specifically larger emitters and smaller collectors, was proposed but unrealistic in application since the voltage capabilities of our power supply was insufficient to induce a corona discharge and hence no measurable result could be found. The 8 different parallel wire configurations were tested with 9 different electrode spacings (2 cm, 4 cm, 6 cm, 8 cm, 10 cm, 15 cm, 20 cm, 25 cm and 30 cm). Using a mill, these spacings were etched into the sides of the PTFE rods. Nylon ratcheting hose clamps were secured about the rods. The



Figure 1 : A picture of our experimental setup. A digital scale is supported by a wooden frame. Suspended from the scale is the hanging testing apparatus which holds the anode and cathode parallel using an insulating PTFE frame.

electrodes were then suspended between two clamps at correspondingly notched a gap distances. Which successfully held the two electrodes parallel and insulated from one another. The Spellman supply was connected to the emitting wire using a properly insulated cable that fed through the supporting frame. The last ~ 10 cm of this cable was a 32 AWG enameled copper wire that was soldered to the emitting wire. The small size and length of wire was chosen to reduce noise in the force measurements incurred by the physical attachment of the power supply to the hanging frame. Similarly, a ~ 15 cm 32 AWG enameled copper wire was soldered to the collector which was connected to a grounded copper braid.

For each gap distance 5-20 different voltages were applied and measured along with the current supplied and the force produced. The small number of differing voltages, at a single gap distance, occurred in instances where the shortness of the gap distance made it difficult to apply voltages that varied largely between each other since the voltage window between corona inception and breakdown was relatively small. The RHR Spellman power supply provided remote monitoring terminals for both voltage and current which is 99% accurate. The current and voltage were measured and displayed on a 5.5 digit 8840A FLUKE multimeter and a 6.5 digit 3547A HP multimeter respectively. The relative uncertainties in each measurement was also documented.

All measurements were recorded on an electronic spreadsheet, then imported and analyzed in MATLAB.

Results and discussion

In an attempt to validate our theory we plotted force and current against voltage and fitted them with equations (4) and (5). In fig. 2 and fig. 3 we display 2 of the unfitted configurations. Through both qualitative and quantitative inspection, we found that equation (4) and (5) held for all 8 configurations. It follows that our assumption of $C \propto \frac{\mu}{d^2}$ holds true. When we began this experiment we desired to find how $C \propto \frac{d_e e}{d_c}$ but this takes several steps of plotting results, fitting results with an equation and then using those fitted coefficients to create a new plot that can be fitted with a different equation. Each subsequent step propagated larger errors, leading to a result that weren't statistically significant. Hence we failed to show how $C \propto \frac{d_e}{d_c}$.

Using an electrode geometry comparable to [4], $d_e = 0.2$ mm and $d_c = 6.4$ mm, we acquired

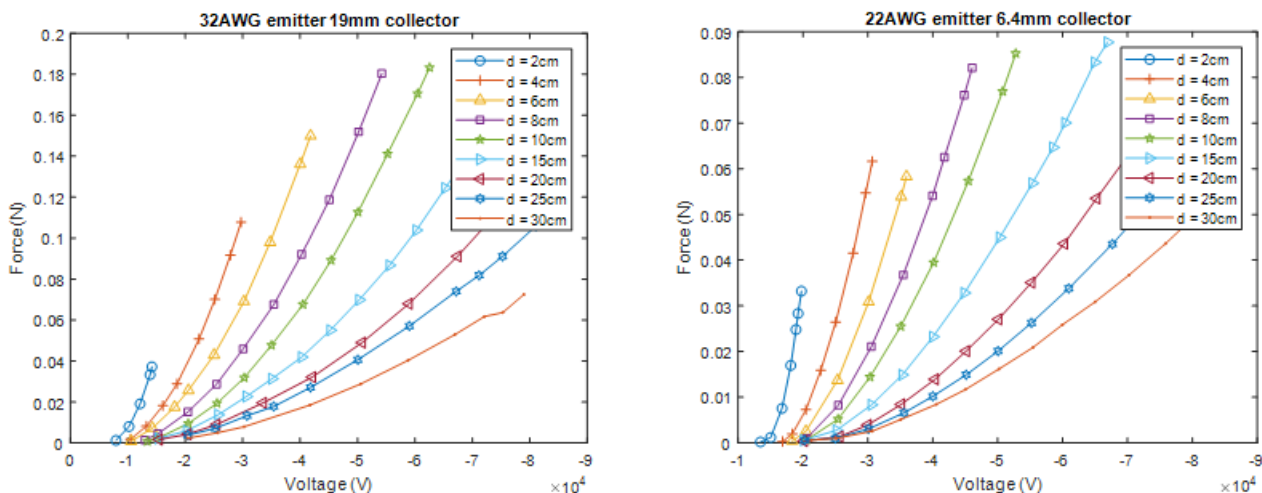


Figure 2 : Force plotted against voltage for 2 different configurations. All 8 configurations follow the model predicted by eq. (5).

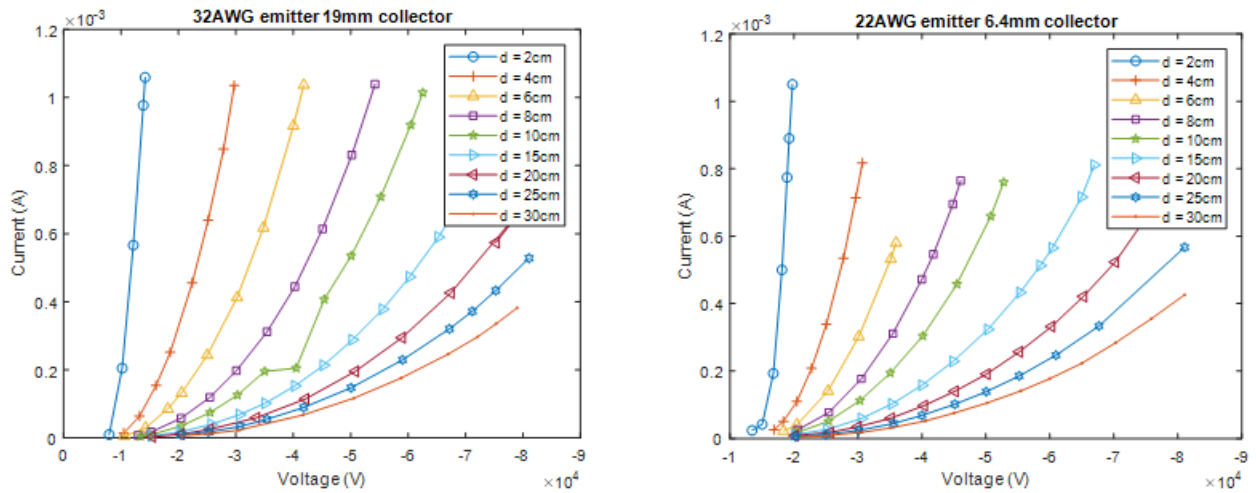


Figure 3 : Current plotted against voltage for 2 different configurations. All 8 configurations follow the model predicted by eq. (4).

results displayed in Fig.4. Masuyama and Barrett reported results that were not predicted by the model at higher gap distances, $d > 9\text{cm}$, and more precisely at $d = 13\text{cm}$ and above, for a given voltage, they saw higher thrust values at larger gap distances. Upon inspection of equation (5), it is clear that for a given voltage the thrust should be lower when the gap distance is larger. Observing fig. 4 we see that our setup obeys the model: the larger the gap distance the thrust is weaker. Furthermore, between the eight F-V spacing comparison plots, none exhibited the anomalous behavior at large gap distances reported by [4]. We may conclude that in our experiment $L \gg d$ holds. Masuyama and Barrett saw the model fail when $d = 13\text{cm}$ with $L = 40\text{cm}$, the electrode spacing to length ratio is 0.325, the largest case ratio we investigated was $d = 30\text{cm}$ with $L = 1\text{m}$ the ratio is 0.3 it is possible the theory $L \gg d$ breaks down somewhere between 0.3 and 0.325 region.

Upon further comparison, we found that our $d = 2\text{cm} - 10\text{cm}$ results reasonably matched Masuyama and Barrett's $d = 1\text{cm} - 9\text{cm}$ results. Beyond this region they reported thrust values that were upwards of 3 times larger than what we observed. This seems to be consistent with the results reported by Monrolin et al., where they found Masuyama and Barrett results to be two times larger than their own. We are inclined to note that the geometries between these experiments are not the same and some of the differences in results can be attributed to this fact. Masuyama and Barrett

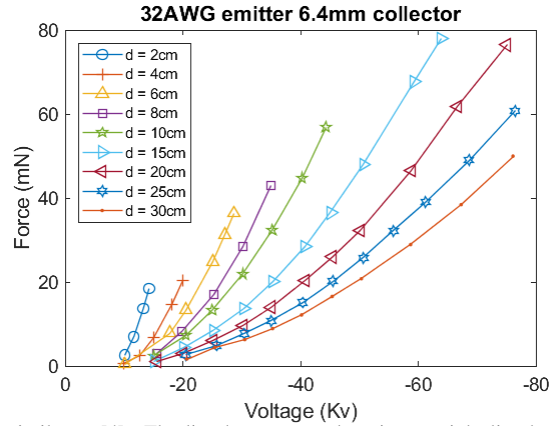


Figure 4 : Results of the setup similar to [4]. The line between markers is a straight line between adjacent points and not a fit. Generally, these results follow the theory associated with equation (5) and aid to show that the extended length of the setup reduces incurred end effects at high gap distances.

used $d_e = 0.2$ mm and $d_c = 6.3$ mm and Monrolin used $d_e = 0.025$ mm, 0.05 mm and $d_c = 3$ mm, 10 mm with distances $d = 2$ cm, 3 cm respectively. Notwithstanding, it is doubtful the large difference between Masuyama and Barrett's results and everyone else's could be attributed to the relatively marginal differences among device geometry.

When analyzing thrust against current, equation (3) states there exists a linear relationship between the two. Applying a fit based on equation (3), for each configuration at each distance, we have extracted several corresponding values of μ . We note that the linear relationship between thrust and current was more prevalent for short electrode gaps than it was for longer gaps. Upon initial experimentation we noticed that as the gap distance got larger there was a greater tendency for the emitter to ignite response from the surroundings, consequently some current that is reported was actually lost to the surrounding interference and not imparted to thrust production. Nevertheless, each μ was statistically significant. Fig. 5 reports the attained μ values and plot them against the gap distance. It was found by [5], for the distances studied ($d = 1$ cm, 1.5 cm, 2 cm, 3 cm, and 4 cm), that the ion mobility decreases as gap distance increases. We see in fig. 5, generally the ion mobility does decrease until about $d = 6$ cm by at which each ion mobility increases. More specifically we see that the increase is separated into two groups: the 6.4 mm collector group and the 19 mm collector group. There is little variation of ion mobility between setups with similar

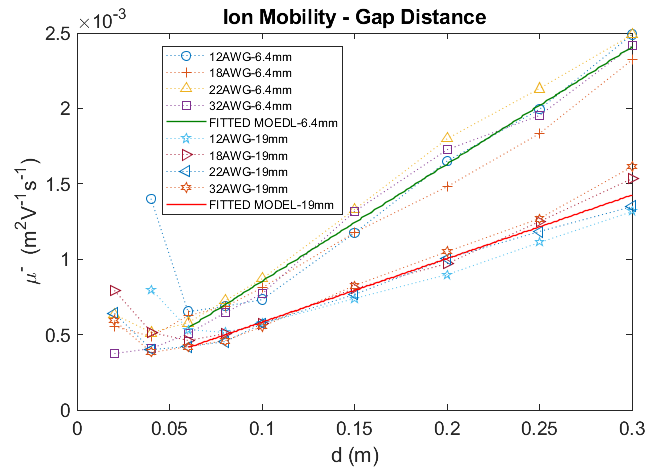


Figure 5 : Ion mobility of each configuration at each tested gap distance is plotted against gap distance. The configurations sort themselves into two consistent groupings for $\approx d > 6$ cm. The top grouping consist of those configurations which used a 6.4 mm collector and the bottom grouping consists of those which used a 19 mm collector. According to equation (3), everything else held equal, the configuration with the smallest μ will result in the highest thrusting device.

collector but differing emitter. We can conclude that when seeking a change in ion mobility, a variation in the collector diameter is more important than a variation in the emitter diameter. And consequently, given all else being the same the 19 mm collector should always produce more thrust than that of the 6.4 mm collector. We also note that this could be used to support the argument made by [2] in which it is claimed that for the region $d < 6$ cm a different mechanism is responsible for initiating thrust than the $d > 6$ cm region. We see the linear relationship for $d > 6$ cm in fig. 5 but for $d < 6$ cm it is generally indiscernible.

Conclusion

We verified equations (3) - (5). Similarly, we confirmed the assumption $C \propto \frac{\mu}{d^2}$, which helped us move from (4) to (5). We note that while current and force both, qualitatively and quantitatively, displayed a quadratic dependence on voltage, a quadratic fit is known to be perfect with only 3 measurements and deviates from there. In some of the lower gap distances we had only 4 viable measurements. Therefore, while the plotted fitted model based on the quadratic fit held closely to the data for these cases, the reported coefficients that built the fitted model had relatively large uncertainties. We would address this problem in a future experiment with 30+ measurements per gap distance.

We found that the increased electrode length eliminated the end effects reported by [4]. While some of our results matched that found by [4], our results deviated significantly from theirs at high gap distances. This discrepancy compounded with a similar discrepancy reported by [9] causes us to question the results reported by [4]. It is possible some other effect could be attributed to their obscure results, but none such contributors were mentioned in their article. Furthermore, we would have to shorten the length of our electrode setup in order to verify [4] and acquire appropriately sized emitters and collectors to properly compare with [9].

We showed that the size of the collector has a larger impact on thrust than the size of the emitter. Our research clearly displays the linear relationship between ion mobility and gap distance, where the configurations linearly grouped according to collector size. This was the most straight forward

method to show how thrust varied according to electrode diameter. While we couldn't obtain an exact numerical model on how thrust depends on electrode size, we were able to determine which electrode was most important.

Bibliography

- [1] M. Robinson, “A History of the Electric Wind,” *Am. J. Phys.* **30**, 366–372 (1962).
- [2] A. Fridman and L. A. Kennedy, in *Plasma Physics and Engineering*, 2 ed., Taylor and Francis, eds., (Taylor and Francis, New York, NY, 2004).
- [3] N. E. Jewell-Larsen, H. Ran, Y. Zhang, M. K. Schwiebert, K. A. H. Tessera, and A. V. Mamishev, “Electrohydrodynamic (EHD) cooled laptop,” In *25th Annual IEEE Semiconductor Thermal Measurement and Management Symposium(San Jose, CA, 2009)*, **25**, 261–266 (IEEE, 2009).
- [4] K. Masuyama and S. Barrett, “On the performance of electrohydrodynamic propulsion,” *Proc R Soc A* **469**, 2154 (2013).
- [5] E. Moreau, N. Bernard, J.-D. Lan-Sun-Luk, and J.-P. Chabriat, “Electrohydrodynamic force produced by a wire-to-cylinder dc corona discharge in air at atmospheric pressure,” *J. Phys. D: Appl. Phys.* **46**, 475204 (2013).
- [6] V. H. Granados, M. J. Pinheiro, and P. A. Sa, “Study of the design and efficiency of single stage EHD thrusters at the sub-atmospheric pressure of 1.3kPa,” *Phys. Plasmas* **24**, 123513 (2017).

- [7] A. A. Martins and M. J. Pinheiro, "On the influence that the ground electrode diameter has in the propulsion efficiency of an asymmetric capacitor in nitrogen gas," *Phys. Plasmas* **18**, 033512 (2011).
- [8] L. Zhao and K. Adamiak, "Numerical analysis of forces in an electrostatic levitation unit," *J. Electrostat* **63**, 729–734 (2005).
- [9] N. Monrolin, F. Plouraboue, and O. Praud, "Electrohydrodynamic Thrust for In-Atmosphere Propulsion," *AIAA* **55**, 12 (2017).
- [10] K. Kiouisis, A. Moronis, and W. Fruh, "Electro-Hydrodynamic (EHD) Thrust Analysis in Wire-Cylinder Electrode Arrangement," *Plasma Sci. Technol.* **16**, 363 (2014).
- [11] D. F. Colas, A. Ferret, D. Z. Pai, D. A. Lactose, and C. O. Laux, "Ionic wind generation by a wire-cylinder-plate corona discharge in air at atmospheric pressure," *J. Appl. Phys.* **108**, 103306 (2010).
- [12] J. Wilson, "An Investigation of Ionic Wind Propulsion," NASA/TM Report 215822 (2009).
- [13] C. Kim, D. Park, K. C. Noh, and J. Hwang, "Velocity and energy conversion efficiency characteristics of ionic wind generator in a multistage configuration," *J. Electrostatics* **68**, 36–41 (2010).